RSC Advances

PAPER

View Article Online
View Journal | View Issue

Cite this: *RSC Adv.*, 2015, **5**, 108002

Rectangular copper nanotubes†

Yu-Hsu Chang,*[a] Ya-Ting Hsu,[a] Yu-Heng Tsai,[a] Yi-Ru Lai,[a] Ting-Kai Huang[b] and Hsin-Tien Chiu[b]

Received 28th August 2015
Accepted 28th November 2015

DOI: 10.1039/c5ra17462g

www.rsc.org/advances

One-dimensional Cu nanomaterials with a new morphology, rectangular copper nanotubes (copper NTs), were synthesized on a large-scale using a cetyltrimethylammonium chloride-assisted galvanic replacement reaction on rough Al substrates. In an acidic environment, Cu(II) is reduced on sharp-topped Al substrates and copper NTs 150–300 nm in diameter and 2–10 μm in length were formed through fine-tuning the reaction temperature and chemical stoichiometry. Field-emission measurement results show that the copper NTs emitting electrons at turn-on fields of 8.76 V μm^{-1} was observed with a field enhancement factor of 85. The superior catalytic property of copper NTs in the degradation of a methylene blue aqueous solution in the presence of H_2O_2 was also presented in this article.

Introduction

One-dimensional (1D) nanostructures, such as nanowires, nanotubes, and nanoribbons, have received considerable attention. Some of these examples include carbon nanotubes,[1–3] silicon nanowires,[4] tellurium nanotubes,[5,6] and zinc oxide nanoribbons.[7,8] Because of the wide potential applications of nanostructures, numerous studies on synthesis methods,[9–13] dimensions and optical properties,[14] surface-enhanced Raman scattering results,[15] and field emission and electrocatalytic properties[16–19] have been published. Metallic copper, silver, and gold feature cubic crystal structures. Therefore, to obtain 1D nanostructures, confined space must be provided to facilitate the anisotropic growth of atomic lattices, which is typically controlled using soft template methods.[20,21] Typically, seed-mediated growth is the most common method used for synthesizing 1D nanostructures.[22] This method applies gold or silver nanoparticles as seeds and a cetyltrimethylammonium bromide surfactant for controlling the product morphology to synthesize gold or silver nanowires or nanorods. Surfactants provide two functions in a reaction.[23] One function involves the surfactant dissolving in an aqueous solution and self-assembling into rod-like micelles. Thus, metal ions can partake in reduction reactions in the template and ultimately form 1D nanomaterial. In the other function, the surfactant acts as a capping agent in crystal plane growth. Because surfactants tend to adsorb on certain facets of metallic atom arrangements, the crystal can only grow in a specific direction, forming rod-like or wire-shaped structures.

In this study, a cetyltrimethylammonium chloride (CTAC) was used as the capping agent to restrict and to control the growth of copper. In addition, a galvanic displacement reaction was induced on the aluminum substrate surface in which the intrinsic potential difference between aluminum (E^0 = 1.66 V) and copper (E^0 = 0.34 V) prompted spontaneous oxidation–reduction reactions. CTAC was used to control the copper growth environment in which the copper ion concentrations, surfactant concentrations, and reaction temperatures were precisely regulated. This method can reduce copper ions into substantial amount of unique 1D rectangular copper nanotubes (copper NTs) on an aluminum substrate. To date, reports on rectangular copper NTs have not yet been published in the literature.

Experimental section

Preparation of Al substrate

According to the literature, high purity aluminum plates (99.999%, Sigma-Aldrich) were electrochemically polished at 20 V to obtain a flat surface.[24] The samples were then placed in a Teflon mold with an O-ring opening of 80 mm^2 where they are anodized in a 0.3 M oxalic acid solution (99.5 wt%, Riedel-deHaën). Subsequently, 6 wt% of phosphoric acid (99.99%, Sigma-Aldrich) was used to remove aluminum oxide. This process was repeated three times. Repeating anodizing processes increases the regularity of previously self-assembled pores, which yields uniformly distributed tips on the aluminum metal surface. An alternative method for creating edgy surfaces is to manually scrape the aluminum substrate by using tweezers. This method can also be applied to prepare the reaction substrate.

[a]*Department of Materials and Mineral Resources Engineering, Institute of Mineral Resources Engineering, National Taipei University of Technology, Taipei 10608, Taiwan, Republic of China. E-mail: yhchang@ntut.edu.tw*

[b]*Department of Applied Chemistry, National Chiao Tung University, Hsinchu 300, Taiwan, Republic of China*

† Electronic supplementary information (ESI) available. See DOI: 10.1039/c5ra17462g

Preparation and characterization of one-dimensional Cu nanostructures

First, 100 mL of 1.8 mM CTAC (99%, Sigma-Aldrich) was prepared to which 22 μL of HNO_3 (69.5 wt%, J. T. Baker) was added. Subsequently, $CuCl_2 \cdot 2H_2O$ powder (99.3 wt%, J. T. Baker) was added into an aqueous solution to prepare a 5 mM $CuCl_2$(aq) solution. After a uniform solution was obtained through magnetic stirring, 20 mL of the reaction solution was placed in a water bath maintained at 21 °C for later use. The prepared aluminum substrates were then placed in the reaction solution to react. The formation of dark red products was observed on the surface of the aluminum substrates over time. After 20 h of reaction, deionized water was added to terminate the reactions. Samples were extracted and blown dry with nitrogen gas. Regarding catalyzed degradation, methylene blue (MB, Sigma-Aldrich)–H_2O_2 (30 wt%, Sigma-Aldrich) at a 2 : 1 volumetric ratio was mixed with 0.01 g copper NTs or copper powders and then allowed to react at room temperature before subjecting to ultraviolet-visible (UV-vis) spectroscopy measurements. The concentrations of MB were determined based on the peak values of $\lambda_{MAX} = 665$ nm. Untreated 3 μm commercial copper powders were used in the control group. The morphologies, chemical compositions and structures of the products were characterized by field-emission scanning electron microscopy (SEM, Hitachi S-4700), energy-dispersive X-ray spectroscopy (EDS), transmission electron microscopy (TEM, JEOL JEM-3000F), powder X-ray diffractometry (XRD, Rigaku DMX-2200, with Cu $K_{\alpha 1}$ radiation, $\lambda = 1.5418 \times 10^{-10}$ m). The photocatalytic properties of the products were characterized by UV-vis spectrometer (PerkinElmer Lambda 900). Current–voltage properties from FE measurements were carried out using a needle-shaped anode with an effective tip-to-sample distance of 65 μm in a vacuum chamber at 4×10^{-6} Torr at room temperature. A positive voltage swept up to 1 kV with a step of 50 V was applied to the anode using a Keithly 2410 power supply.

Results and discussion

Al substrate preparation

Through precisely controlled anodizing processes, ordered hexagonal structures were self-assembled on the surface of the aluminum plates. The basal alumina and aluminum surfaces formed multiple pointy tips. Rough aluminum surfaces were obtained by dissolving away close-packed, ordered, and porous hexagonal channels, as shown in Fig. 1a. In addition, a rough surface can be obtained by manually scratching the surface of the aluminum plates by using tweezers. The resulting plates can also be used as the reaction substrates, as shown in Fig. 1b. Atomic force and optical microscopy images showed that numerous tips were successfully created on the aluminum surfaces. Despite a lack of orderliness, these two types of substrates can be employed in subsequent reactions.

Synthesis of rectangular copper nanotubes

When the reaction temperature and $CuCl_2$ concentration were precisely controlled at 21 °C and 5 mM, respectively, numerous copper NTs exhibiting novel morphologies were successfully synthesized. EDS analysis revealed that the nanosized products were primarily composed of copper with traces of oxygen and carbon. SEM images (Fig. 2a) showed substantial copper NTs on the aluminum substrate surface, indicating a considerably high yield. Fig. 2c shows a high-magnification SEM image that clearly illustrates the morphology of the copper NTs. The overall appearance presents hollow rectangular structures with measured widths, thicknesses, and lengths of approximately 300–400 nm, 30–50 nm, and several micrometers, respectively. Fig. 2b indicates that few of the copper NT products exhibited solid centers and needle-like openings;[25] however, most of the products were hollow rectangular structures.

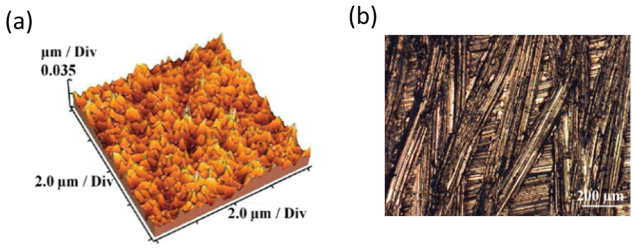

Fig. 1 (a) AFM topography and (b) optical microscope image of rough Al substrate.

Fig. 3 shows the SEM image of the copper NTs synthesized when the $CuCl_2$(aq) concentration was reduced to 3.5 mM. This equally yielded numerous elongated copper NTs with side lengths and thicknesses of approximately 200–300 and 30–50 nm, respectively, suggesting that the copper NT dimensions can be fine-tuned by changing the Cu ion concentrations. XRD analysis revealed that (Fig. S1†) signals appeared at $2\theta = 43.3°$ and 50.5°, which were representative of the (111) and (200) face-centered cubic (FCC) copper crystal planes. The lattice constant was $a = 0.361$ nm, which matched that of metallic copper (Powder Diffraction Files by the Joint Committee on Powder Diffraction Standards; JCPDF 04-0836; $a = 0.362$). The XRD data subsequently confirmed that the hollow structured products on the aluminum substrates were FCC copper.

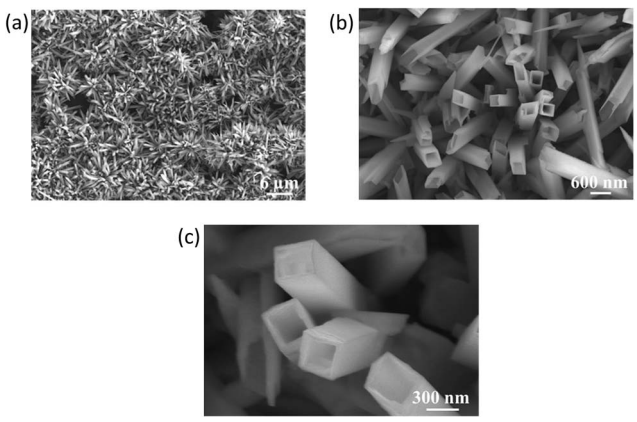

Fig. 2 SEM images of copper NTs at different magnifications. The concentration of $CuCl_2$ in the reaction is 5 mM.

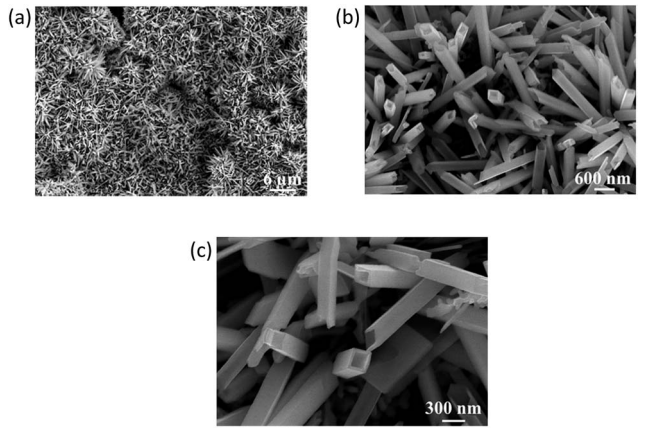

Fig. 3 SEM images of copper NTs at different magnifications. The concentration of $CuCl_2$ in the reaction is 3.5 mM.

A TEM image (Fig. 4a) of a copper NT synthesized at 21 °C showed that the first half portion of the 1D nanostructures comprised solid-centered copper nanowires, which gradually formed into hollow tube structures in the second half portion of the nanostructure. The tube structures were externally covered by an apparent layer of substance. To identify this microstructure, high-resolution TEM and selected area electron diffraction (SAED) were applied. SAED showed that the *d*-spacings of 0.208, 0.181, 0.128, and 0.109 nm represented the FCC Cu (111), (200), (220), and (311) crystal planes, respectively. The 1D growth direction was [100], and lattice spacing was 0.244 nm, which belongs to the Cu_2O (111) crystal plane (JCPDF 04-0667). These measurements confirmed that the hollow tube material was the typical FCC metallic copper structure, which exhibited Cu_2O oxidized on the copper surface by contact with air and water.

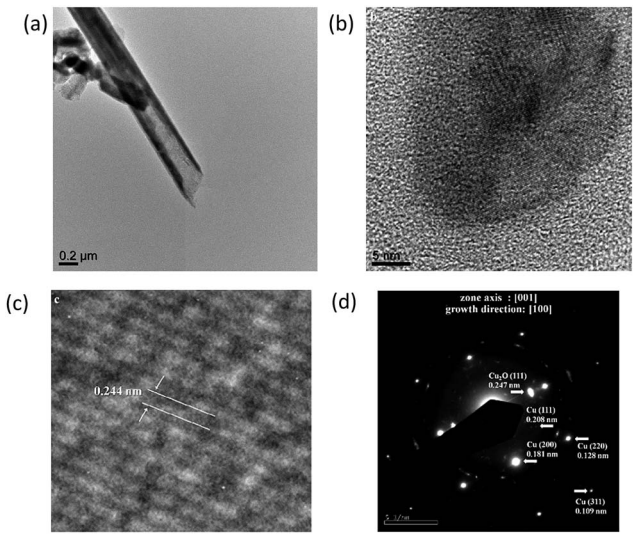

Fig. 4 (a) Copper NTs TEM image showing the hollow structure; (b and c) HRTEM images taken from the edge of copper NT and the lattice fringes revealing the Cu_2O (111) planes, separated by 0.244 nm; (d) electron diffraction patterns showing FCC Cu and Cu_2O crystal planes.

To observe the influence of $CuCl_2$ concentration on morphologies, all synthesized copper NTs were separately reacted again in 5 mM and 3.5 mM of $CuCl_2$–CTAC solutions for 20 h. During the second reaction in 5 mM of $CuCl_2$(aq), the hollow tubes were filled forming rectangular copper nanorods (copper NRs) of side lengths ranging from approximately 300 to 500 nm (Fig. 5a and b). During the second reaction in 3.5 mM of $CuCl_2$(aq), the product morphologies comprised sealed-rectangular copper NTs (closed copper tube ends) in addition to the rectangular columnar structures. The results indicated that, during the second reaction, Cu^{2+} ions continued to reduce on the copper NTs and fill the interspace, forming columnar structures. When the concentration was 3.5 mM, the available Cu^{2+} was less abundant and the tubes remained hollow within, which yielded partially hollow, closed tube structures (Fig. 5c and d). In addition, sealed-rectangular cooper NTs featured unique structures. The optimal synthesis environment and microstructural analyses are currently underway. Scaled and uniformed products are anticipated by fine-tuning the synthesis conditions.

In most studies, hard templates, such as anodic aluminum oxides, have been adopted for synthesizing metallic nanotubes. In addition, plating solution concentrations and voltages have been adjusted for controlling the morphology of the final products to form nanotube structures.[25] However, this study proposes a novel synthesis method that applies a surfactant-assisted reduction reaction to prepare nanotube structures. In the reaction system, when CTAC dissolved in water, Cl^- anions first adsorbed on the copper surface before adsorbing on the positively charged CTA^+. Because of the van der Waals force between the molecules at the terminal end of long carbon chains, the CTAC self-assembled into bilayer structures as a soft template.[23,26] The TEM and electron diffraction analyses invalidated the (100) plane as the tightly packed crystal plane after the adsorption of CTAC. Therefore, Cu^{2+} ions tend to reduce and deposit on the Cu (100) orientation, growing into a 1D structure. The CTAC concentrations added were less than the critical micelle concentration in the reactions; therefore, the possibility of an advanced surfactant micelle formation inducing 1D

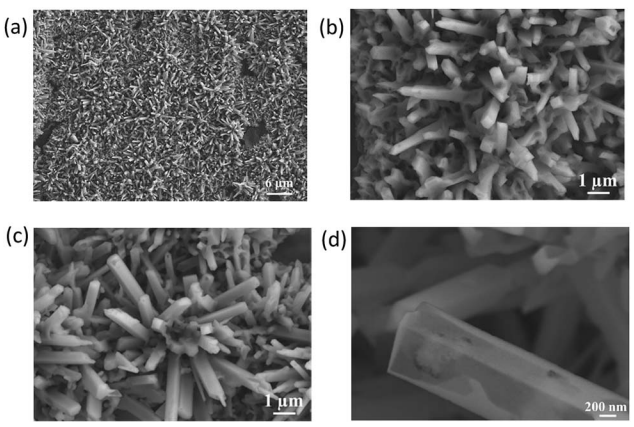

Fig. 5 SEM images of synthesized copper NTs grown again in (a and b) 5 mM and (c and d) 3.5 mM of $CuCl_2$ solutions for 20 h.

growth was eliminated. Through a series of experiments, the ratio between $CuCl_2$ and CTAC concentrations must be precisely controlled to form tube-like products. When CTAC concentrations are inadequate, insufficient capping agents are provided for adsorption on the copper surface. When CTAC concentrations are in excess, micelles are formed and CTAC molecules no longer selectively adsorb on various crystal planes; therefore, 1D copper growth cannot be controlled.

In addition, a series of experiments and observations were conducted on the formation of the tube-like structures. At the initial stage of the reaction, sufficient concentrations of Cu^{2+} were provided in the system for copper formation. The added effect of surfactants caused copper NRs to form. At the late stages of the reaction, Cu^{2+} concentrations decreased, CTAC self-assembled at the 4 edges and provided limited space for Cu growth. Therefore, tube structures were formed at the late stages of the reaction. The SEM images showed needle-like openings on some of the copper NTs, which could be caused by the relatively high current densities at the four edges that caused the tips to discharge electricity. This effect was suggested as one of the reasons facilitating the formation of the tube structures. Therefore, toward the end of the reaction, inadequate Cu^{2+} were available for reduction, prompting the metallic copper to grow into nanotube structures along the four edges in the [100] direction. Fig. 6 illustrates the growth mechanism.

Filed emission property

One-dimensional metallic nanomaterial typically exhibit excellent field emission properties; therefore, these properties were measured for the copper NT samples. Because copper easily oxidizes when exposed to the atmosphere, the samples were quickly washed, blown dry with nitrogen gas, and placed into a vacuum chamber within 1 min following the completion of the reaction. Fig. 7a shows the current density (J)–electric field (E) diagram of the copper NTs. The diagram indicates that the current densities reached the minimum field emission standard of 10^{-6} mA cm^{-2}. Field emission properties can be expressed using the Fowler–Nordheim equation.[27] The calculations yielded a turn-on voltage and field enhancement factor (β)

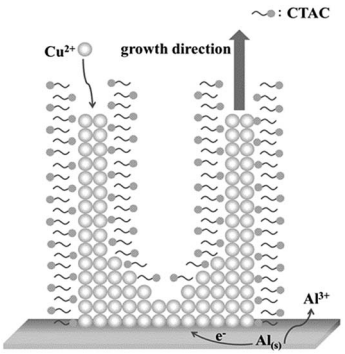

Fig. 6 Schematic representation of rectangular copper NTs growth *via* CTAC-assisted galvanic replacement reaction on rough Al substrate.

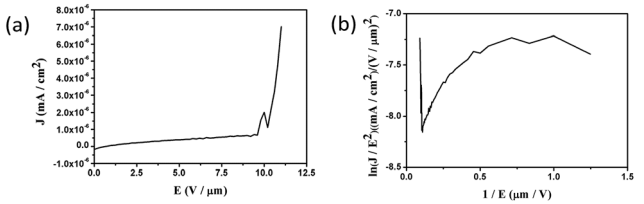

Fig. 7 (a) Emission current density as a function of the applied electric field on copper NTs (b) corresponding FN.

of 8.76 μm^{-1} and 85, respectively, which confirmed the excellent field emission properties of the copper NTs.

Catalytic property

Copper or copper oxide exhibits favorable catalytic properties in chemical industrial applications.[28–32] The surfaces of the copper NTs synthesized in this study formed oxide layers because of atmospheric contact. Moreover, the hollow structure substantially increased the microstructural surface areas. These characteristics were used to examine the effect of adopting copper NTs for catalyzing degradation tests of MB using H_2O_2. Fig. 8a shows the absorption intensities with respect to time from UV-vis spectroscopy for MBs in solutions that contained H_2O_2 and copper NTs. The diagram clearly indicates that the MB absorption peak is located at 655 nm in which the intensity progressively diminished over time. This represents the complete degradation of MB in the solutions. Fig. 8b shows the degree of degradation with respect to time. $(I_0 - I)/I_0$ was used to calculate the degree of degradation, where I_0 and I denote the absorption intensities at $t = 0$ and reaction time t, respectively. The results revealed that the degradation of MB using strictly H_2O_2 reached 35% after 13 h of reaction. When copper NTs (synthesized using 5 mM of $CuCl_2$) was used to catalyze degradation, the reactions completed within 8 h. When copper NTs synthesized using 3.5 mM of $CuCl_2$–CTAB was used, 90% degradation was reached 8 h into the reaction. In another control group experiment in which H_2O_2–commercial copper powder was adopted to catalyze degradation, no catalytic effects were observed on the degradation of MB. During the reaction process, MB and H_2O_2 adsorbed on the metallic copper surface. H_2O_2 decomposed into highly oxidative free radicals, promoting the oxidation and decomposition of MB, which desorbs from

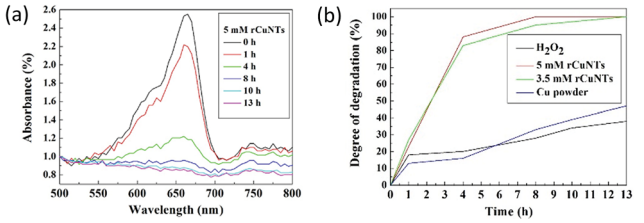

Fig. 8 (a) Absorption spectra with respect to time for MBs in solutions containing H_2O_2 and copper NTs. (b) Time profiles of MBs in solutions containing H_2O_2, H_2O_2 + copper NTs or H_2O_2 + commercial Cu powders.

the copper nanostructures into small molecules. The hollow structures of copper NTs present large surface areas when compared with typical commercial copper powders and easily promote adsorption–oxidation–desorption reactions, thereby providing excellent degradation abilities.

Conclusions

In this study, a straight-forward galvanic displacement reaction in the aqueous phase was adopted to synthesize structurally novel copper NTs. Roughening the aluminum substrate surface substantially increased the yield of 1D copper nanostructures. The CTAC surfactant acted as a capping agent during the crystal plane growth in the experiment. Selective adsorption on the surface of the copper restricted crystal growth and guided the growth of 1D hollow structures. This 1D copper nanomaterial consisted of excellent field emission properties and exerted favorable catalytic effect in H_2O_2 solutions on the degradation of MB. Regarding the synthesis conditions, the product morphology can be fine-tuned under a certain range of conditions. For example, reactant dosage variations may yield differing copper tube diameters. Second reactions may yield rectangular copper NRs or sealed-rectangular copper NTs. Furthermore, reaction temperature is key to tailoring the diameters of copper NRs (to be published) when controlled between 17 and 19 °C.

Acknowledgements

The authors thank the Ministry of Science and Technology of Taiwan, ROC (NSC-99-2113-M-027-003) and National Taipei University of Technology for financial support.

References

1 S. Iijima and T. Ichihashi, *Nature*, 1993, **363**, 603.
2 R. J. Baughman, A. A. Zakhidov and W. A. de Heer, *Science*, 2002, **297**, 787.
3 Z. F. Ren, Z. P. Huang, J. W. Xu, J. H. Wang, P. Bush, M. P. Siegal and P. N. Provencio, *Science*, 1998, **282**, 1105.
4 A. M. Morales and C. M. Lieber, *Science*, 1998, **279**, 208.
5 M. Mo, J. Zeng, X. Liu, W. Yu, S. Zhang and Y. Qian, *Adv. Mater.*, 2002, **14**, 1658.
6 B. Mayers and Y. Xia, *Adv. Mater.*, 2002, **14**, 279.
7 Z. W. Pan, Z. R. Dai and Z. L. Wang, *Science*, 2001, **291**, 1947.
8 X. Y. Kong and Z. L. Wang, *Nano Lett.*, 2003, **3**, 1625.
9 J. Hu, T. W. Odom and C. M. Lieber, *Acc. Chem. Res.*, 1999, **32**, 435.
10 J. Choi, G. Sauer, K. Nielsch, R. B. Wehrspohn and U. Gösele, *Chem. Mater.*, 2003, **15**, 776.
11 Y. Xiong, H. Cai, B. J. Wiley, J. Wang, M. J. Kim and Y. Xia, *J. Am. Chem. Soc.*, 2007, **129**, 3665.
12 C.-H. Hsia, M.-Y. Yen, C.-C. Lin, H.-T. Chiu and C.-Y. Lee, *J. Am. Chem. Soc.*, 2003, **125**, 9940.
13 M.-Y. Yen, C.-W. Chiu, C.-H. Hsia, F.-R. Chen, J.-J. Kai, C.-Y. Lee and H.-T. Chiu, *Adv. Mater.*, 2003, **15**, 235.
14 C. J. Murphy, T. K. Sau, A. M. Gole, C. J. Orendorff, J. Gao, L. Gou, S. E. Hunyadi and T. J. Li, *J. Phys. Chem. B*, 2005, **109**, 13857.
15 B. J. Wiley, Y. Chen, J. M. McLellan, Y. Xiong, Z.-Y. Li, D. Ginger and Y. Xia, *Nano Lett.*, 2007, **7**, 1032.
16 J. Hernandez, J. Solla-Gullon, E. Herrero, A. Aldaz and J. M. Feliu, *J. Phys. Chem. B*, 2005, **109**, 12651.
17 A. Dangwal, C. S. Pandey, G. Müller, S. Karim, T. W. Cornelius and C. Trautmann, *Appl. Phys. Lett.*, 2008, **92**, 063115.
18 J.-H. Wang, T.-H. Yang, W.-W. Wu, L.-J. Chen, C.-H. Chen and C.-J. Chu, *Nanotechnology*, 2006, **17**, 719.
19 C. Kim, W. Gu, M. Briceno, I. M. Robertson, H. Choi and K. Kim, *Adv. Mater.*, 2008, **20**, 1859.
20 A. Filankembo and M. P. Pileni, *J. Phys. Chem. B*, 2000, **104**, 5865.
21 I.-C. Chang, T.-K. Huang, H.-K. Lin, Y.-F. Tzeng, C.-W. Peng, F.-M. Pan, C.-Y. Lee and H.-T. Chiu, *ACS Appl. Mater. Interfaces*, 2009, **1**, 1375.
22 C. J. Murphy and N. R. Jana, *Adv. Mater.*, 2002, **14**, 80.
23 J. Gao, C. M. Bender and C. J. Murphy, *Langmuir*, 2003, **19**, 9065.
24 O. Jessensky, F. Müller and U. Gösele, *Appl. Phys. Lett.*, 1998, **72**, 1173.
25 H.-W. Wang, C.-F. Shieh, H.-Y. Chen, W.-C. Shiu, B. Russo and G. Cao, *Nanotechnology*, 2006, **17**, 2689.
26 B. Nikoobakht and M. A. El-Sayed, *Langmuir*, 2001, **17**, 6368.
27 R. H. Fowler and L. W. Nordheim, *Proc. R. Soc. London, Ser. A*, 1928, **119**, 173.
28 L. Xu, S. Sithambaram, Y. Zhang, C.-H. Chen, L. Jin, R. Joesten and S. L. Suib, *Chem. Mater.*, 2009, **21**, 1253.
29 M. Yang and J. He, *J. Colloid Interface Sci.*, 2011, **355**, 15.
30 X. Liu, F. Li, H. Wang, J. Yang, Z. Li, Y. Wang and H. Jin, *J. Nanosci. Nanotechnol.*, 2014, **14**, 4108.
31 T. Kou, C. Jin, C. Zhang, J. Sun and Z. Zhang, *RSC Adv.*, 2012, **2**, 12636.
32 D. Jana and G. de, *RSC Adv.*, 2012, **2**, 9606.

